LAWRENCE
LIVERMORE
NATIONAL
LABORATORY

LLNL-CONF-450383

# Development of 10B2O3 processing for use as a neutron conversion material

L. F. Voss, J. Oiler, A. M. Conway, R. T. Graff, C. E. Reinhardt, Q. Shao, T. F. Wang, R. J. Nikolic

August 20, 2010

World Materials Research Institutes Forum: Workshop for Young Materials Scientists
Berlin, Germany
August 31, 2010 through September 3, 2010

## Disclaimer

Development of $^{10}B_2O_3$ processing for use as a neutron conversion material

L.F. Voss, J. Oiler, A.M. Conway, R.T. Graff, C.E. Reinhardt, Q. Shao, T. F. Wang, and R.J. Nikolic

Lawrence Livermore National Laboratory

Livermore, CA 94550

ABSTRACT

Development of thermal neutron detectors is critical for a number of homeland security and physics applications. In this work, we describe our efforts towards developing boron-10 oxide ($^{10}B_2O_3$) as a thermal neutron conversion material for textured PIN silicon pillar diode platforms. The filling of the textured diode was achieved by first infiltrating the structures with aqueous boric acid, followed by thermal annealing at above the melting point of boron oxide to achieve a high fill and conversion of the materials into boron oxide. The present solution phase processing strategy has the potential to yield amenable and economical manufacturing processes for coating neutron converter materials on detectors. Potential performance of a boron oxide filled detector is also discussed.

INTRODUCTION

Interest in thermal neutron detectors has increased significantly over the past several years in response to heightened fears of nuclear proliferation and terrorism. The application space for thermal neutron detectors is broad. Reliable detectors are needed in a large number of form factors with different size and performance requirements. Currently, $^{3}$He filled gas tubes are the standard for thermal neutron detection the in field. In response to the diminishing supply of available $^{3}$He and the rapidly increasing demand for thermal neutron detectors, a number of technologies are being explored. These include boron-10- ($^{10}$B) lined gaseous tubes, boron-10-triflouride ($^{10}BF_3$) -filled tubes, lithium-6- ($^{6}$Li) doped scintillators, and other semiconductor based platforms utilizing $^{6}$Li [1-4], $^{10}$B or $^{10}$B containing compounds [5-10] such as boron nitride, boron carbide [11] and boron phosphide. Our group has been developing a 3-dimenstional (3d) Si based "Pillar Detector," first reported in 2005 by Nikolic et al [8] with $^{10}$B as the thermal neutron conversion material. This approach relies on pure $^{10}$B deposited by low pressure chemical vapor deposition (LPCVD )[10], and has achieved detectors with 20% intrinsic detection efficiency [9], with the possibility to increase to greater than 50%. McGregor et al. have developed a design based on $^{6}$LiF in perforations, also a promising approach based on a 3d geometry.[1-4] Typically, thermal neutron detectors operate on similar principles, relying on an isotope with a high thermal neutron cross-section such as $^{3}$He, $^{10}$B, $^{6}$Li, $^{157}$Gd and $^{113}$Cd. An incident thermal neutron interacts with the neutron sensitive material, resulting in a nuclear reaction. The products are then either directly collected or converted to electron-hole pairs in a semiconductor, or photons in a scintillator.

The use of a semiconductor based system offers several advantages over gas filled tube based detectors. First, since a solid neutron converter material is used instead of a gas, this allows a significantly smaller detector footprint for solid state detector devices. In addition, a solid detector offers the potential for superior fieldability due to their decreased sensitivity to vibrations, ease of

transport compared to gaseous chambers, and potential for lower voltage operation. In the initial development of solid state detectors, the semiconductor based detectors were based on a flat diode coated with a thin film of neutron conversion material. However, due to inherent limitations in this type of design, the maximum efficiency for detectors with a single conversion layer design is about 4%. [1] Recently, our group has reported on a three dimensional solution which has the potential to achieve >50% efficiency [9]. Having a non-vacuum based deposition method is attractive from a process cost-reduction and complexity standpoint. In this work, we report on the use of $^{10}B_2O_3$ as a potential neutron converter material within our 3D pillar structure.

## THERMAL NEUTRON CONVERSION IN BORON OXIDE

Semiconductor based thermal neutron detectors typically go through a three-step detection process (Figure 1a). In the first step, a thermal neutron collides with the neutron conversion material and creates several nuclear or charged particles and gamma rays. In the second step, these charged products deposit their energy in the semiconductor detector in the form of electron-hole pairs. The third step is the collection of these pairs to generate a detectable signal.

In order to determine whether a detector design based on $^{10}B_2O_3$ can feasibly achieve a high intrinsic efficiency , we have calculated the probability of neutron capture for $^{10}B_2O_3$ films of varying thickness . $^{10}B_2O_3$ has a $^{10}B$ atomic density of only 33.8% that of pure $^{10}B$ solid, 0.723 g/cm$^3$ compared to 2.13 g/cm$^3$. This translates to an increase in neutron mean free path (λ) from 18 μm to 53 μm. To determine the effect of this on the thermal neutron efficiency for homeland security purposes, it must be noted that thermal neutrons to be detected in this case are not strictly directional. This is because neutrons are expected to be emitted at high energies from special nuclear materials and only become thermalized as they are moderated in the surrounding environment. Figure 2a shows that we have opted to calculate efficiency based on a 4π distribution of thermal neutrons, or neutrons incident on the

detector equally from all directions and at all angles. Figure 2b displays the neutron capture probability vs incident angle for $^{10}B_2O_3$films of varying thickness. From this, it is clear that a significant fraction of the incident neutrons can be captured only for sufficiently thick coatings. Because our pillar structure relies on interspersed Si p-i-n diodes to overcome the limitation on coating thickness imposed by the Li and alpha travel lengths, we have calculated the path lengths of these particles in $^{10}B_2O_3$ using "Transport of Ions in Matter" (TRIM), shown in Table 1. These are similar to the pillar spacing and pitch (2 μm and 4 μm, respectively) we have previously fabricated and reported for our $^{10}B$ filled devices. We find that a thickness of >70 μm is needed to capture 85% of the neutrons incident on a film, compared to >95% capture for a 50 μm $^{10}B$ film.

## FABRICATION OF BORON OXIDE FILLED PILLAR ARRAY

One advantage of semiconductor based detectors is that their development can draw on the extremely strong knowledge developed in the integrated circuit industry. To process our devices, we exploit common semiconductor manufacturing processing tools and techniques including photolithographically defined patterns, dry plasma and wet chemical etching, lapping and polishing of materials, and sputter or e-beam deposition of electrodes. The major challenges to achieving these detectors include etching pillars to sufficient height, achieving a high degree of filling of pillars with $^{10}B_2O_3$, and processing the $^{10}B_2O_3$ after fill in order to deposit electrodes and insulate it from the environment. The last item is particularly important. Since $^{10}B_2O_3$ is hygroscopic, it converts to $H_3{}^{10}BO_3$ when exposed to humidity and dissolves readily in a large array of polar solvents such as water and methanol.

Silicon pillar array platforms are defined using standard photolithographic techniques. To achieve the aspect ratios required, we employ nLOF 2035 negative photoresist, which produces a mask of ~2.8 μm in thickness. Etching is done in an STS DRIE Bosch system, using a process recipe composed

of alternating fluorobutante ($C_4F_8$) sidewall passivation and sulfur hexafluoride ($SF_6$) silicon etch steps [8]. Erosion of the photoresist mask is a potentially serious problem if the selectivity is not carefully controlled; an overall etch selectivity of >25:1 must be achieved to produce silicon pillar arrays of greater than 75 µm. In addition, care must be taken not to overestimate the selectivity due to highly aspect-ratio-dependent etching. Also, the sidewall slope of the pillars must be nearly vertical for our device design. For an array consisting of 2-µm wide pillar with a height of >50 µm, even slight positive or negative tapers can result in pinching off of the etch or undercut of the pillar leading to insufficiently tall pillars or collapse of the pillars, respectively. We have achieved >70 µm tall pillars with photoresist remaining on top. Figure 3 shows a cross-sectional scanning electron microscopy (SEM) image of these as-processed pillars.

*Solution based deposition of $^{10}B_2O_3$*

Filling such high aspect ratio structures presents a challenge. Common solid source deposition techniques, such as sputtering and e-beam evaporation, generally do not achieve a reasonable fill due to pinching off or shadowing effects at the tops of the pillars. While gaseous chemical vapor deposition is possible and has produced excellent results for our $^{10}B$ detectors [5-10], material precursors and deposition equipment can be expensive. As an alternative, we have developed processing capabilities to deliver $^{10}B_2O_3$ via a solution-based process to achieve near 100% fill.

$^{10}B_2O_3$ is unique among compounds containing a high boron percentage. It is soluble in a variety of benign polar solvents and is extremely hygroscopic. $^{10}B_2O_3$ kept under normal room conditions will inevitably convert to $H_3{}^{10}BO_3$. Fortunately, this process can be reversed upon heating, forming several intermediate compounds depending on the temperature, as shown below.

$H_3BO_3$ -> $HBO_2$ + $H_2O$ (433K)

$4HBO_2$ -> $H_2B_4O_7$ + $H_2O$ (573K)

$H_2B_4O_7$ -> $2B_2O_3$ + $H_2O$ (Further heating)

In addition, $B_2O_3$ has a relatively low melting temperature, 450°C, which is low enough to minimize doping of the Si pillars by B diffusion. For comparison, boron implanted in silicon is generally activated using rapid thermal annealing (RTA) at temperatures greater than 1000K. Nonetheless, merely piling on powder and heating the $^{10}B_2O_3$ to 450°C cannot be applied to fill our pillar arrays because it will result in limited infiltration of the pillar structure (Fig 4).

Our strategy to achieve a high degree of filling of $^{10}B_2O_3$ in our pillar array structures is to dissolve the $^{10}B_2O_3$ in a solvent in order to infiltrate the pillar structure. In our process, $^{10}B_2O_3$ powder is added to methanol until saturation. The solution mixture is then delivered by pipettes to coat the pillar structured chips. The methanol is allowed to evaporate off entirely under normal room temperature conditions. No extra immediate heat is supplied to the samples because rapid evaporation and/or boiling of the methanol can result in broken pillars. The chip is then inserted into a furnace, subsequently heated to between 450°C and 510°C. After this heat treatment, Raman spectroscopy study is applied to the samples to confirm the presence of $^{10}B_2O_3$ and absence of $H_3{}^{10}BO_3$ (Figure 5). The Raman peak present at ~805 $cm^{-1}$ indicates B-O bonds [12], while that at ~880 $cm^{-1}$ indicates the O-H bonds indicative of $H_3BO_3$ [13]. Note the absence of the latter after heat treatment. Some indication exists that temperatures >500°C lead to reaction of the $^{10}B_2O_3$ with Si, with possible by-products such as $SiO_2$, Si-B compounds, and borosilicates [14]. Though we have observed reductions in pillar size at annealing temperatures larger than 600 °C, no appreciable sample shrinkage effect is found at 500°C, even when held at this temperature for longer than 24 hours. Figure 6a shows a pillar chip of 25-μm height coated with $^{10}B_2O_3$ at 500°C. Figure 6b shows the risk of increasing the annealing temperature. In this case, the sample was heated to 700°C. Note that the pillars have nearly completely dissolved into the surrounding $^{10}B_2O_3$. The “bulbs” on the tops of some pillars are a result of incomplete fill. These areas of silicon have not come into prolonged contact with the surrounding $^{10}B_2O_3$ and so have not reacted. We have also performed filling of $^{10}B_2O_3$ on 50-μm pillar chips with similar success.

*Etching of $^{10}B_2O_3$*

A serious challenge to the use of $^{10}B_2O_3$in a detector is developing the capability to planarize the coating for further electrode deposition processing. Our detector requires a blanket metal contact on top of the pillars. The $^{10}B_2O_3$ coating that we deposit results in an uneven over-filled coating on the top of the pillars; the excess material must be removed with a method that does not attack the underlying Si pillars should they become exposed. Both wet and dry etching techniques are unsuitable for this task because neither will return a flat surface. However, most dry etching recipes that remove $^{10}B_2O_3$ will almost certainly attack the underlying Si. We have opted to develop a process to mechanically etch the $^{10}B_2O_3$. By utilizing a gentle enough polish, the underlying Si should not be damaged. In addition, since higher elevation features are removed faster than lower ones, it should be possible to achieve a final planar final surface for electrode deposition.

Chemical-mechanical planarization (CMP) is a common method for removing overfill of both ductile materials (i.e. metals) [15-16] and brittle materials such as $SiO_2$ [17]. In addition, it has previously been used to remove borosilicate glass, which generally contains ~13% $B_2O_3$. However, solutions for etching borosilicate glass are water-based; these etchants rely on hydrolyzing the silicon dioxide for weakening the structure [18], rather than the $B_2O_3$. When exposed to a water-based solution or slurry, the $B_2O_3$ begins to dissolve immediately and cracks grow within the oxide fill. Therefore, we have opted to use silicone oil. By using 0.3 µm size grit, a spin speed of 50 rpm, we achieved a $^{10}B_2O_3$ removal rate of *ca.* 1.5 µm/min. This is a very fast etch rate considering this compound is typically used as a polishing etch which has a neglible etch rate for most group IV and III-V semicondcutors. This, however, results in infiltration of the $Al_2O_3$ grit into the pillar structure, replacing the $^{10}B_2O_3$, shown in Figure 7a. This can be avoided by polishing only with a polishing pad and a small amount of silicone oil.

Figure 7b shows a SEM image of a fully etched surface. Electrode deposition and device testing on these boron oxide filled structures are currently in progress.

## SUMMARY

We demonstrated that boron oxide can be used within our 3d Pillar Platform using a solution based process for the fabrication of thermal neutron detectors. Upon evaluating the composition of $^{10}B_2O_3$, and mean free path of neutrons within this material, capture of a significant number of neutrons can be achieved with pillar height in excess of 70 µm . A simple polishing solution of silicon oil with 0.3 micron "polish grit" is also developed to achieve an etch rate of 1.5 µm /min of $^{10}B_2O_3$for planarization of our structures after the boron oxide deposition process. Further work on $^{10}B_2O_3$ encapsulation is currently being pursued to minimize the dissolution of boron oxide under humid environment.

## ACKNOWLEDGEMENTS

This work was performed under the auspices of the U.S. Department of Energy by Lawrence Livermore National Laboratory under Contract DE-AC52-07NA27344, LLNL-xxxx. This work was supported by the Domestic Nuclear Detection Office in the Department of Homeland Security.

REFERENCES


1. D. S. McGregor, R. T. Klann, H. K. Gersch and Y. H. Yang, Nucl. Instrum. Methods Phys. Res. A **466** (1), 126-141 (2001).
2. D. S. McGregor, R. T. Klann, H. K. Gersch, E. Ariesanti, J. D. Sanders and B. Van Der Elzen, IEEE Trans. Nucl. Sci. **49**, 1999-2004 (2002).
3. J.K. Shultis and D. S. McGregor, IEEE Trans. on Nucl. Sci. **53** (3), 1659-1665 (2006).
4. J.K. Shultis and D.S. McGregor, Nucl. Instrum. Methods Phys. Res. A 606 (3), 608-636 (2009).
5. A. M. Conway, R. J. Nikolic and T. F. Wang, International Semiconductor Device Research Conference, College Park, MD, December 12-14, 2007.
6. R. J. Nikolic, A. M. Conway, C. E. Reinhardt, R. T. Graff, T. F. Wang, N. Deo and C. L. Cheung, International Conference on Solid State and Integrated Circuit Technology, Beijing, China, October 20-23, 2008.
7. R. J. Nikolic, C. L. Cheung, C. E. Reinhardt and T. F. Wang, International Symposium on Integrated Optoelectronic Devices, 6013 (1), 36-44 (2005).
8. R. J. Nikolic, A. M. Conway, C. E. Reinhardt, R. T. Graff, T. F. Wang, N. Deo and C. L. Cheung, Appl. Phys. Lett. 93, 133502 (2008).
9. A. M . Conway, L. F. Voss, C. E. Reinhardt, R. T. Graff, T. F. Wang, N. Deo, C. L. Cheung, and R. J. Nikolic, CMOS Emerging Technologies Conference, February 2009.
10. Deo, N., Brewer, J.R., Reinhardt, C.E., Nikolić, R.J. and Cheung, C.L, J. Vac. Sci. Technol. B, 26, 1309-1314 (2008).
11. K. Osberg, N. Schemm, S. Balkir, J. I. Brand, M. S. Hallbeck, P. A. Dowben and M. W. Hoffman, IEEE Sensors J. **6** (6), 1531-1538 (2006).
12. D. Maniu, T. Iliescu, I. Ardelean, S. Cinta-Pinzaru, N. Tarcea, and W. Kiefer, J. Mol. Struct. 651 (1), 485 (2003).
13. R. R. Servoss and H. M. Clark, J. Chem. Phys. 26 (5), 1175 (1957).
14. E. De Fresart, S. S. Rhee, and K. L. Wang, Appl. Phys. Lett. 49, p. 847, 1986.
15. Li, X., Abe, T., Liu, Y., and Esashi, M., J. Microelectromechanical Systems, 11, 625-630, (2002).
16. Todd, S.T., Huang, X.T., Bowers, J.E., and MacDonald, N.C., J. Microelectromechanical Systems, 19, 55-63 (2010).
17. Davarik, B., Koburger, C.W., Schulz, R., Warnock, J.D., Furukawa, T., Jost, M., Taur, Y., Schwittek, W.G., DeBrosse, J.K., Kerbaugh, M.L., Mauer, J.L., Electron Devices Meeting, 1989, 61–64 (1989).
18. Oliver, M.R. (Ed.), Chemical-Mechanical Planarization of Semiconductor Materials, Springer-Verlag, Berlin Heidelberg, 2004.

LIST OF TABLES

Table 1

| | 1.47 MeV Alpha | 0.84 MeV Li |
|---|---|---|
| $^{10}B_2O_3$ | 3.5um | 1.89um |

Voss et al.

LIST OF FIGURES

Figure 1

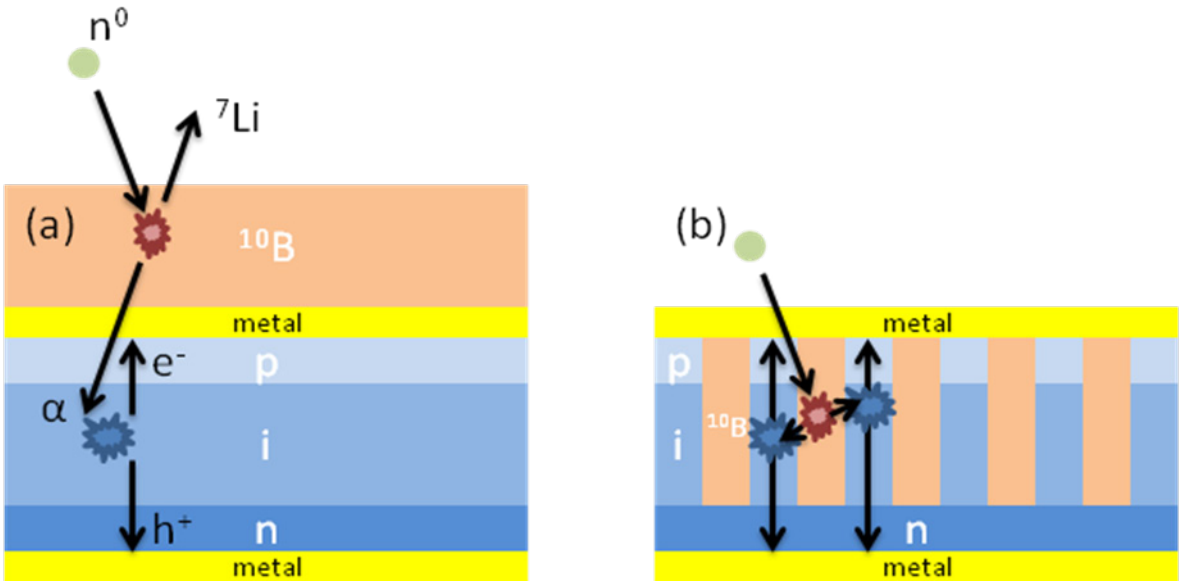


Voss et al

Figure 2

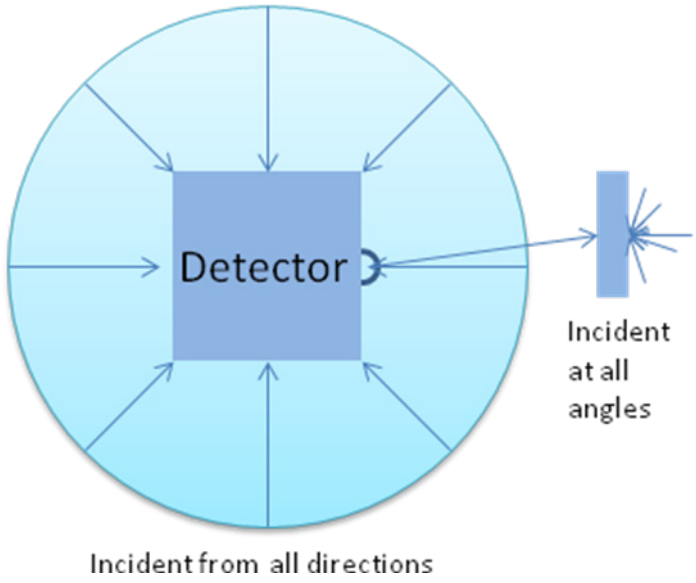
Detector
Incident at all angles
Incident from all directions

(a)

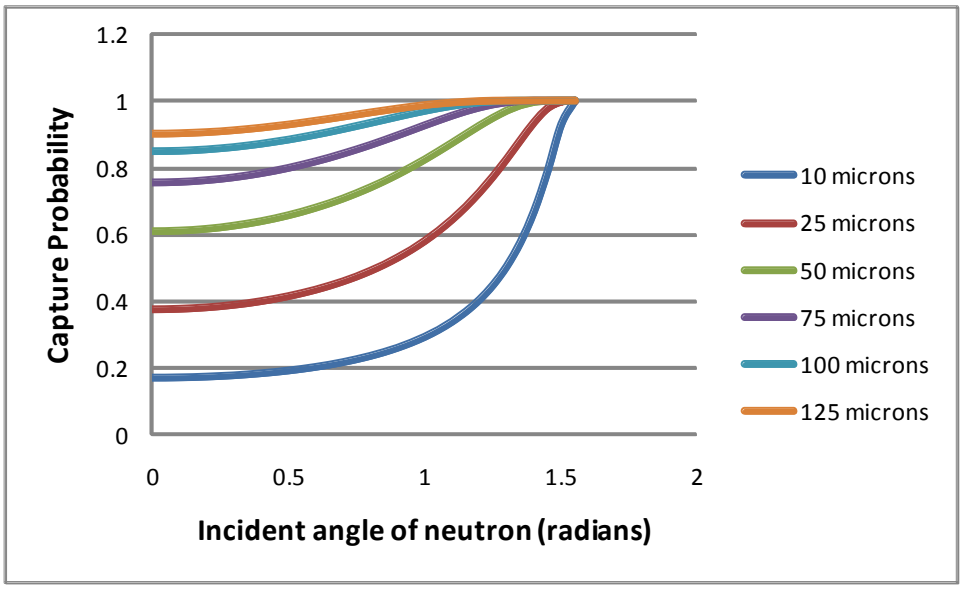
Capture Probability
1.2
1
0.8
0.6
0.4
0.2
0
0
0.5
1
1.5
2
Incident angle of neutron (radians)
10 microns
25 microns
50 microns
75 microns
100 microns
125 microns

(b)

Figure 3

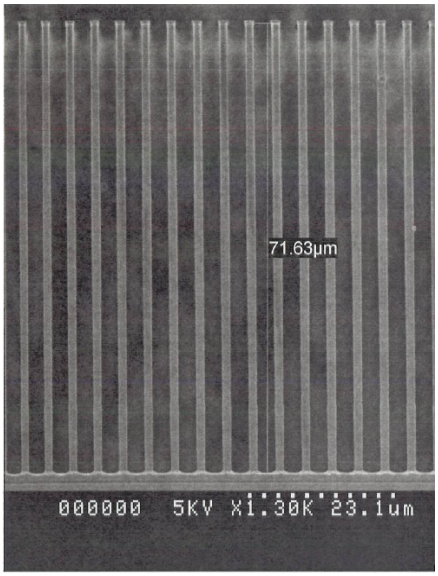


Voss et al.

Figure 4

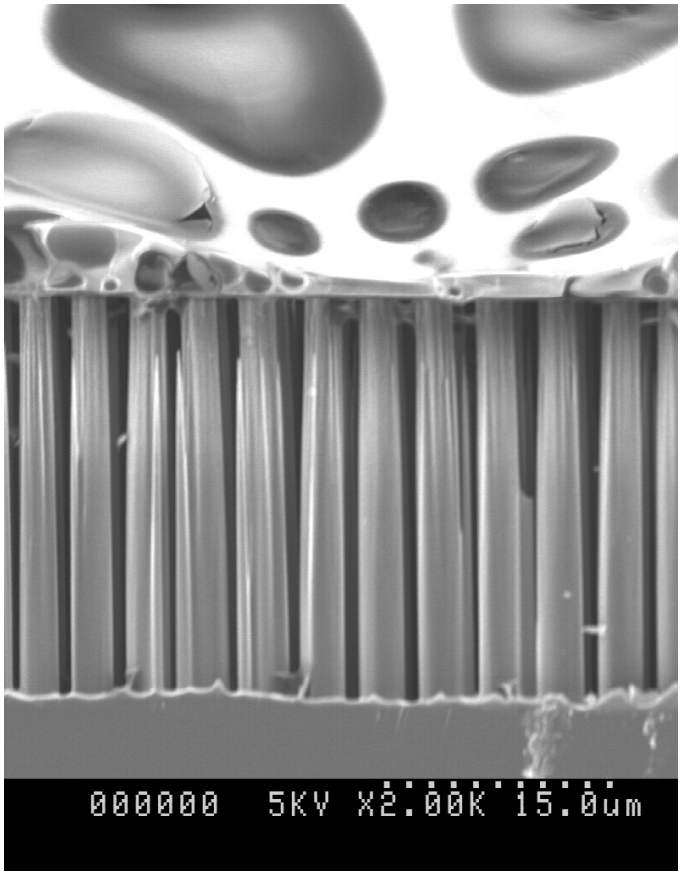


Voss et al.

Figure 5

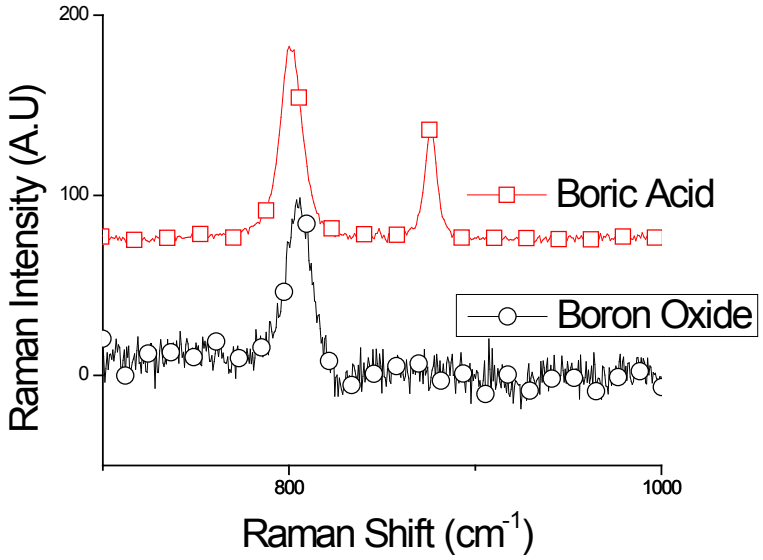


Voss et al.

Figure 6

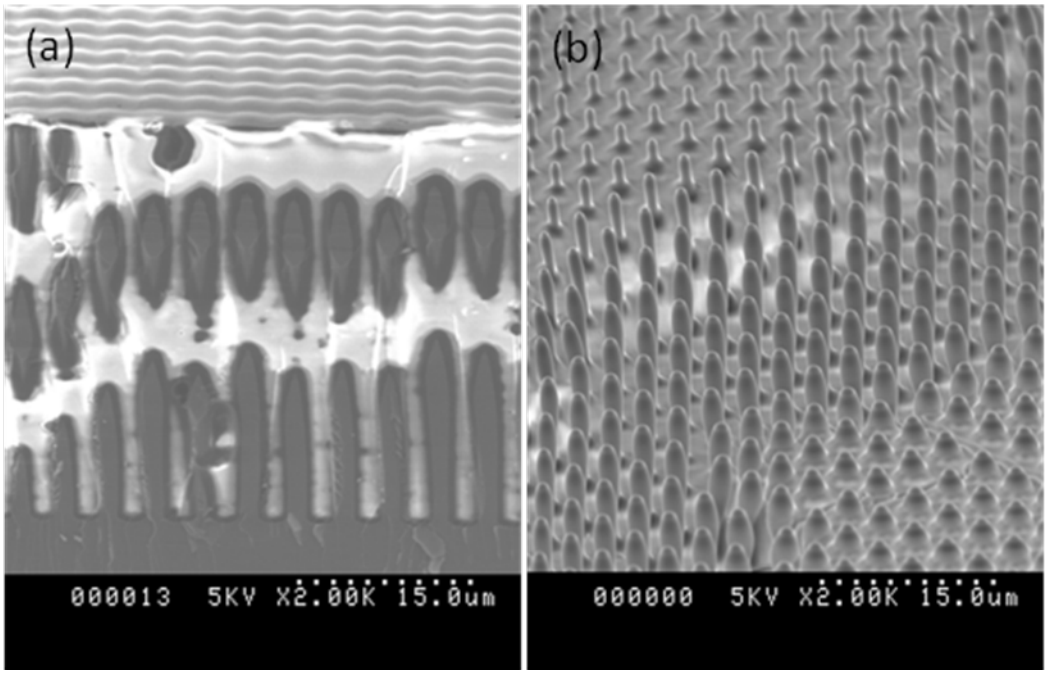


Voss et al.

Figure 7

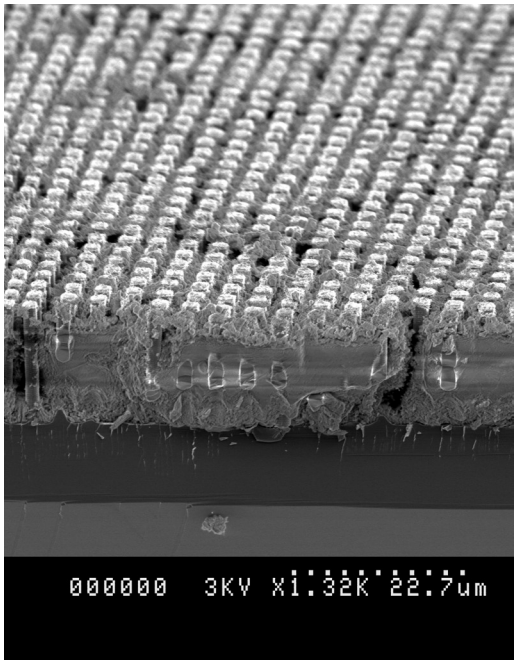


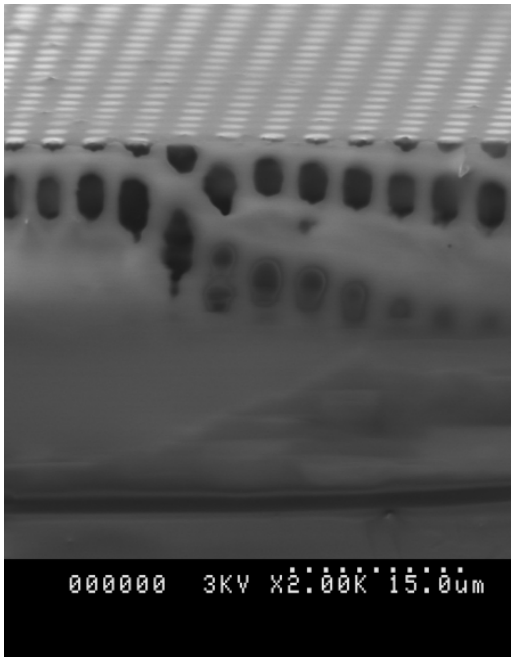


Voss et al.